Sonochemistry and Sonodynamic Therapy: Spin Trapping and EPR Studies

Joe Z. Sostaric and Peter Riesz

Room B3-B69, Bldg 10
Radiation Biology Branch
Center for Cancer Research
National Cancer Institute
National Institutes of Health
9000 Rockville Pike
Bethesda MD 20814-1002

phone: (310) 496-4036
fax: (301) 480-2238
Dr. Riesz e-mail: sono@helix.nih.gov
Dr. Sostaric e-mail sostarij@mail.nih.gov

Introduction to Acoustic Cavitation and Sonochemistry

- Sonochemistry:chemical effects of ultrasound on aqueous and non-aqueous solutions. The effects are due to Acoustic Cavitation: the nucleation, growth and violent collapse of gas/vapor filled microbubbles in a liquid.
- The widely accepted Hot Spot Theory proposes that collapse of these microbubbles is an almost adiabatic process.
- This results in the creation of very high temperatures (thousands of Kelvin) and pressures (hundreds of atmospheres) in extremely small and transient regions in the liquid (Hot Spots).
- The collapse of bubbles is accompanied by the simultaneous emission of light (Sonoluminescence).
- This presentation describes the detection of radical species produced as a result of acoustic cavitation in aqueous solutions.

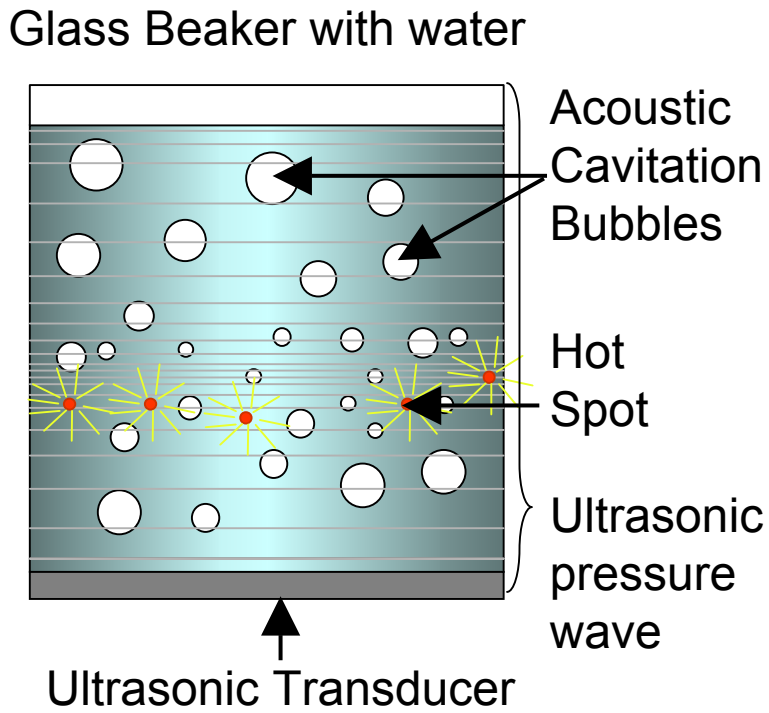

Experimental Set-up:

- To identify free radicals generated by ultrasound, suitable spin traps were added to the sample solution before sonolysis. The stable spin adducts were identified by EPR immediately after sonolysis.
- Recently, we have employed a more sophisticated experimental set-up to study radical formation after sonolysis at various ultrasound frequencies and intensities. Temperature control should be employed for extended sonolysis times or high ultrasound intensities.

Figure 1: Apparatus purchased from L3-Communications - ELAC Nautik GmbH, Germany.

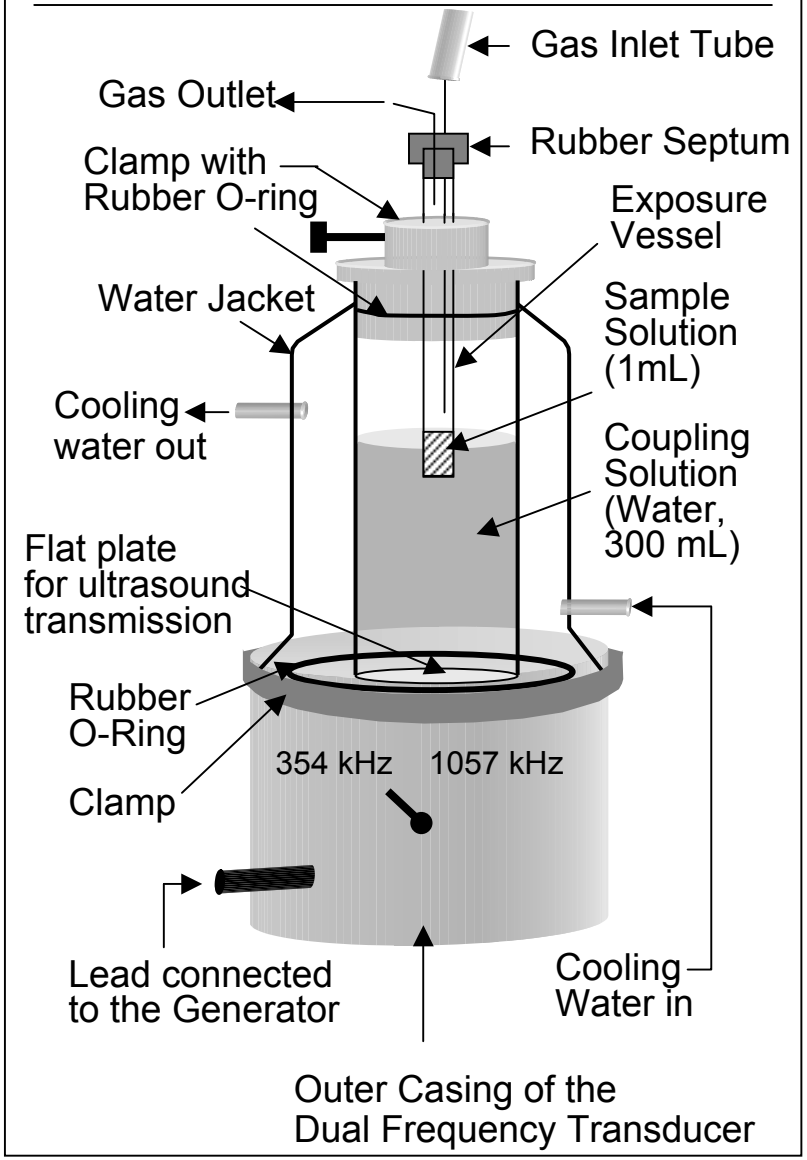

Acoustic Cavitation:

i) *Characteristics of the Ultrasonic Wave*:

Ultrasound travels through a liquid as a longitudinal wave, i.e., the molecules of the liquid oscillate about their equilibrium positions in the direction of the motion of the wave. Therefore, the effective pressure in any given region of liquid is determined by the equation, $P_t = P_h + P_a$, where P_t = the total pressure in a specific region in the liquid, P_h = the hydrostatic pressure and P_a = the acoustic pressure in a particular region and time.

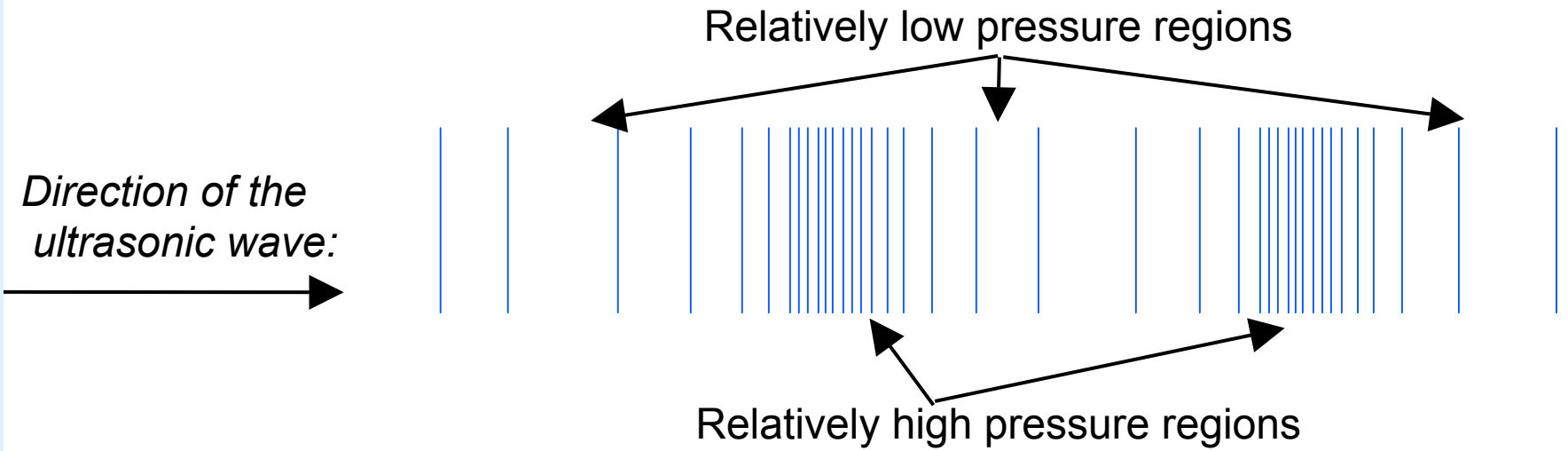

Figure 2: Pressure effects in the liquid due to an ultrasonic wave.

ii) *Nucleation, Growth and Collapse of Microbubbles:*

- Pockets of gas are trapped on microscopic impurities (e.g., dust particles), inherently present in any liquid, or in imperfections on the wall of the vessel.
- The gas nuclei expand under the influence of the ultrasonic wave and detach to form free microbubbles in the liquid. The microbubbles continue to adsorb energy from the wave and grow isothermally.
- When the microbubbles reach a critical size (approximately 2 to 3 times the resonance radius), they implode violently. Assuming adiabatic collapse, the temperature of the hot spot can be estimated using the equation below. This equation demonstrates the importance of γ in determining the collapse temperature (note, the collapse is not completely adiabatic, so the thermal conductivity will effect T_f in a real system).

$$T_f = T_i \left(\frac{R_{max}}{R_{min}} \right)^{3(\gamma-1)}$$

Where, T_f is the temperature of the core, T_i is ambient temperature, R_{max} and R_{min} are the maximum and minimum bubble radius and γ is the ratio of specific heats (C_p/C_v) of the gas inside the bubble. γ = 1.67 for monoatomic gases and 1.40 for diatomic gases.

Figure 3: The Sonochemical Hot Spot*

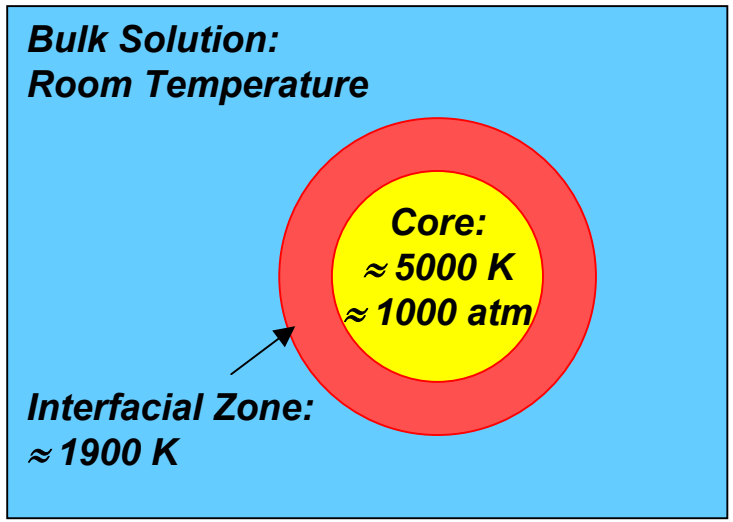

*Suslick, K.S. et al., *J. Am. Chem. Soc.*, **1986**, *108*, 5641.

Sonochemistry

i) *The Three Regions of Chemical Activity:*

Sonochemical reactions can occur in three different regions.

Region 1: interior of collapsing gas bubbles (i.e., the core) in which very high temperatures and pressures exist. Under these conditions the solvent vapor inside the bubble undergoes pyrolysis reactions.

Region 2: interface between the collapsing bubble and the bulk solvent, where high temperature and pressure gradients exist. In aqueous solutions, the relative efficiency of non-volatile solutes to decompose thermally or to scavenge radicals formed in the hot spot depends on their ability to accumulate at the gas/solution interface of the growing microbubble.

Region 3: bulk solution at ambient temperature. Free radicals formed in the hot regions may diffuse to the bulk solution and react to yield products similar to those found in aqueous radiation chemistry. Thus, sonochemistry can partly be understood in terms of a combination of combustion chemistry and radiation chemistry.

ii) *Spin Trapping and EPR Following Sonolysis of Liquids:*

It is well known that volatile and/or surface active solutes can thermally decompose in the core of the hot spot or in the hot interfacial zone. These factors must be considered in choosing the spin trap for detection of radicals formed during sonolysis. The following slides illustrate the choice and use of various spin traps in sonochemistry.

Spin-Trapping during the Sonolysis of Aqueous Solutions

i) *Important Characteristics of the Spin Trap:*

Spin traps with greater hydrophobicity and/or volatility thermally decompose more readily in the hot interfacial zone or in the core of the hot spot. An example of this is shown in the figure below.

Because, in general, alkyl radicals react much faster with aromatic nitroso spin traps than with nitrone spin traps, DBNBS-d_2 could be used to identify the carbon centered radicals produced following decomposition of a number of spin traps. The figure below shows the methyl radical yield following sonolysis of spin traps as a function of solute concentration.

The hydrophobicity of the spin traps follows the order NPBN > PBN > POBN > SPBN.
The greater the hydrophobicity of the spin trap, the lower the spin trap concentration at which radicals can be observed.

Figure 4: $^{\bullet}CH_3$ yield as a function of the bulk concentration of spin traps of varying hydrophobicities.

NPBN = α-(4-nitrophenyl) *N-tert*-butylnitrone
PBN = α-phenyl-*N-tert*-butylnitrone
POBN = α-(4-pyridyl-1-oxide) *N-tert*-butylnitrone
SPBN = α-(2-sulfophenyl) *N-tert*-butylnitrone

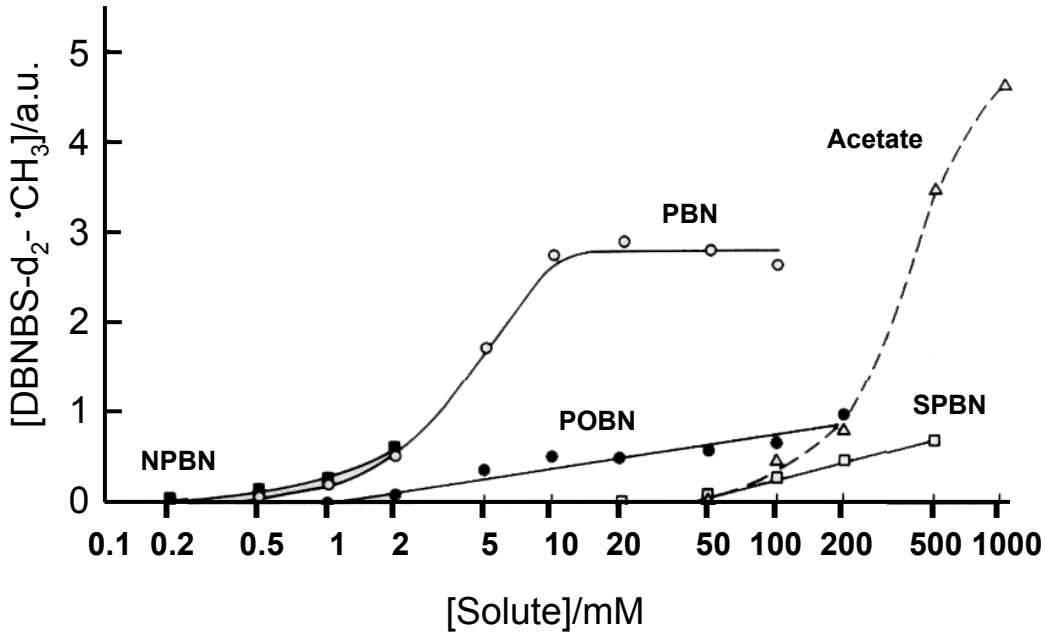

Kondo, T.; Riesz, P.; *Free Radic. Biol. Med.*, **1989**, *7*, 259-268.

ii) *Probing the Temperatures of the Hot Spot:*

- The semi-classical model of the temperature dependence of the kinetic isotope effect for •H and •D atom formation was used to estimate the effective temperature of the hot cavitation region in which •H and •D atoms are formed by ultrasound-induced pyrolysis of water molecules.
- For example, the ratio of •H/ •D could be determined by spin trapping of •H and •D atoms from a 1:1 molar mixture of H_2O:D_2O in the presence of POBN (10 mM). The ratio of •H/ •D = k_H/k_D = 1.20 ± 0.06, which corresponds to a hot spot temperature of between 2600 K to 4600 K, using: $k_H/k_D = \exp\{(1.24 \text{ kcal mol}^{-1})/RT\}$

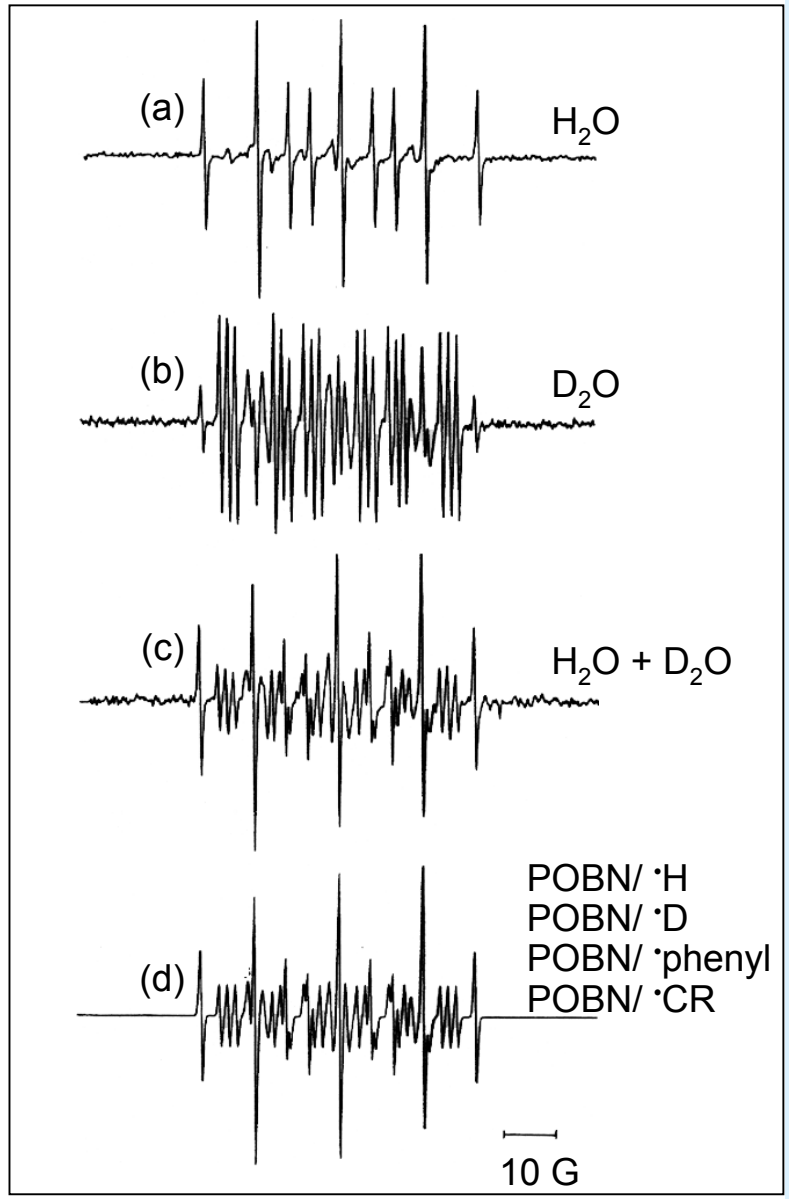

Figure 5: EPR Spectra of spin adducts produced by sonolysis of argon-saturated (a) H_2O; (b) D_2O; (c) 1:1 molar H_2O:D_2O. (d) is a computer simulation of (c). The species that contribute to the spectrum in (c) are shown in (d).

Misik, V.; Miyoshi, N.; Riesz, P; *J. Phys. Chem.*, **1995**, *99* (11), 3605-3611.

iii) *Identifying the Primary Species during the Sonolysis of Argon Saturated Water*

Using the spin trap DMPO, EPR spectra characteristic of the $^{\bullet}H$/ $^{\bullet}OH$ - DMPO spin adducts were observed following the sonolysis of water. Assignment was confirmed by using other $^{\bullet}OH$ radical scavengers and isotopically labeled water (D_2O and H_2O^{17}). Other nitrone spin traps (PBN, POBN and PYBN) were also used.

For example, the EPR spectrum (a) obtained by sonolysis of an aqueous, argon saturated POBN solution (25 mM) resulted in the formation of the $^{\bullet}H$-POBN adduct, as illustrated by the stick diagram. The life-time of the $^{\bullet}OH$-POBN adduct is too short to be detected using the conventional EPR technique. In order to show that $^{\bullet}H$-POBN adducts were formed by trapping of $^{\bullet}H$ atoms, we added well known $^{\bullet}H$ atom (and $^{\bullet}OH$) scavengers during sonolysis in the presence of POBN.

In Figure 6(b), the addition of the formate ion (5.2 M) to solution resulted in an EPR spectrum due to the $^{\bullet}CO_2^-$-POBN spin adduct, following the scavenging of $^{\bullet}H$ atoms (and $^{\bullet}OH$ radicals) by HCO_2^-.

Finally, sonolysis of D_2O solutions under the same conditions resulted in the formation of $^{\bullet}D$-POBN, spectrum (c). The small amount of $^{\bullet}H$-POBN in spectrum (c) is due to the decomposition of POBN.

Figure 6: Spectra obtained following sonolysis of POBN (25 mM) in water (a and b) and (c) D_2O.

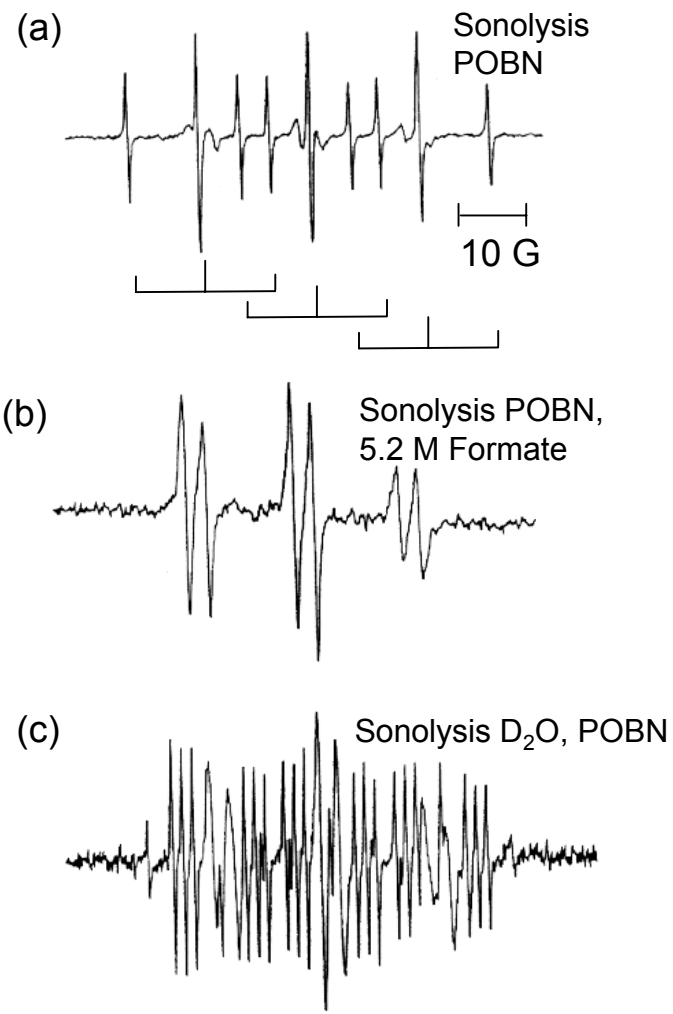

Makino, K; Mossoba, M. M.; Riesz, P. *J. Phys. Chem.*, **1983**, *87* (8), 1369-1377.

iv) *Evidence Against Formation of Hydrated Electrons during Sonolysis of Water:*

It has been proposed that the formation of hydrated electrons occurs following the exposure of aqueous solutions to ultrasound (Margulis M. A. (1995) Sonochemistry and Cavitation, Gordon and Breach Publishers, Luxembourg).

Cadmium ions (Cd^{2+}) are efficient scavengers of hydrated electrons, but do not react with $^{\bullet}H$ atoms. Therefore, the effect of Cd^{2+} on the $^{\bullet}D$-POBN yield following sonolysis of D_2O solutions (shown in Figure 6) was investigated.

D_2O was used to avoid any errors due $^{\bullet}H$ atom formation from the decomposition of POBN during sonolysis.

Figure 7 shows that the $^{\bullet}D$-POBN yield is independent of the Cd^{2+} concentration (up to 0.1 M), where 98.8 % of hydrated electrons would be scavenged by Cd^{2+}.

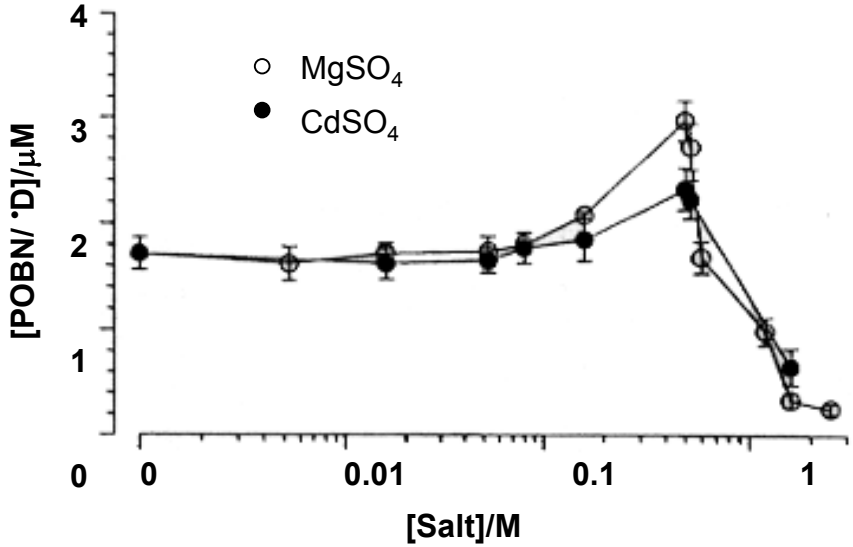

Figure 7: Effect of salt concentration on the yield of POBN/D following sonolysis of argon saturated solutions.

The sharp rise and subsequent decrease in the D-POBN yield at concentrations of $CdSO_4$ > 0.1 M were also observed with the addition of $MgSO_4$.

This effect may be due to a number of phenomena which are observed during the sonochemistry of high salt concentration solutions. However, any observed changes at $CdSO_4$ concentration > 0.1 M are not relevant for the discussion of the possibility of the existence of hydrated electrons.

Misik, V.; Riesz, P. *J. Phys. Chem. A*, **1997**, *101*(8), 1441-1444.

v) *Detection of Radicals from Aqueous Surfactant Solutions:*

Addition of surface active organic solutes to aqueous solutions can result in dramatic enhancements in the chemical reactivity observed during sonolysis, especially through enhanced redox and radical reactions occurring in the bulk solution. These effects can be attributed to the preferential accumulation of the surfactants at the gas/solution interface of cavitation bubbles:

Figure 8: Collapsing Cavitation Bubble

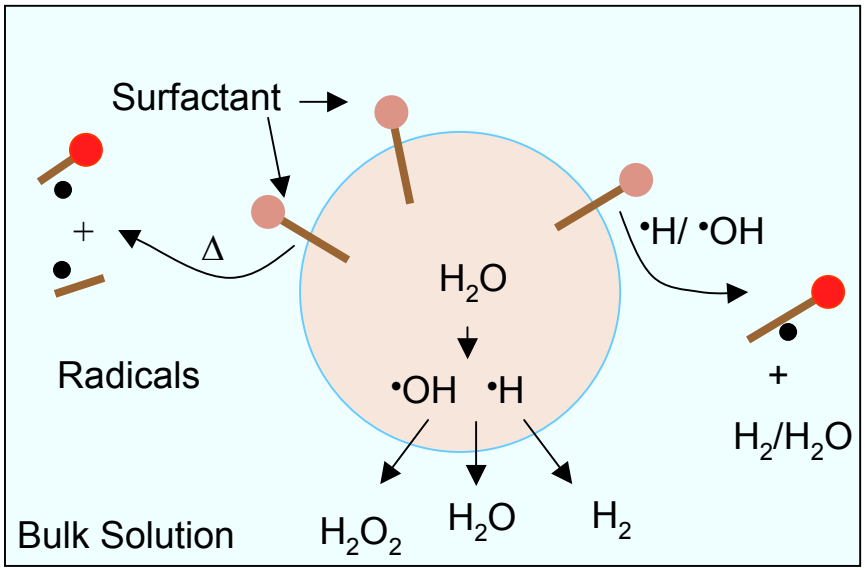

Organic surfactant molecules can scavenge the primary •H atoms and •OH radicals at the gas/solution interface. This has at least two effects. First, it creates relatively long-lived carbon radicals that can diffuse into the bulk solution to react with other solute molecules. Secondly, the radical scavenging reaction of •H/ •OH with the surfactant is in competition with radical recombination reactions which produce non-reactive species such as H_2 and H_2O.

The non-volatile surfactants can also thermally decompose at the hot interfacial zone of the hot spot. This results in the formation of methyl and other carbon centered radicals that are derived from the homolysis of C-C bonds.

Preferential accumulation of surfactants at the gas/solution interface of cavitation bubbles was shown to occur by spin trapping with DBNBS-d_2. Sonolysis of aqueous solutions of a homologous series of non-volatile n-alkyl glucopyranosides [methyl (MGP), n-octyl (OGP) and n-decyl (DGP)]* was conducted in the presence of DBNBS as the spin trap. •CH radicals (formed by abstraction reactions - e.g., Figure 8) and methyl radicals (formed by pyrolysis of the non-volatile surfactants at the gas/solution interface of cavitation bubbles) were observed. An example of the EPR spectrum observed following sonolysis of OGP in the presence of DBNBS-d_2 and argon gas is shown in Figure 9a, which is typical of the spectra observed for all of the glucopyranosides. A simulation of the spectrum in Figure 9a is shown in Figure 9b. The simulation shows that the acquired EPR spectrum can be interpreted in terms of contributions from methyl (•CH_3), primary (- •CH_2), secondary (- •CH-) and tertiary

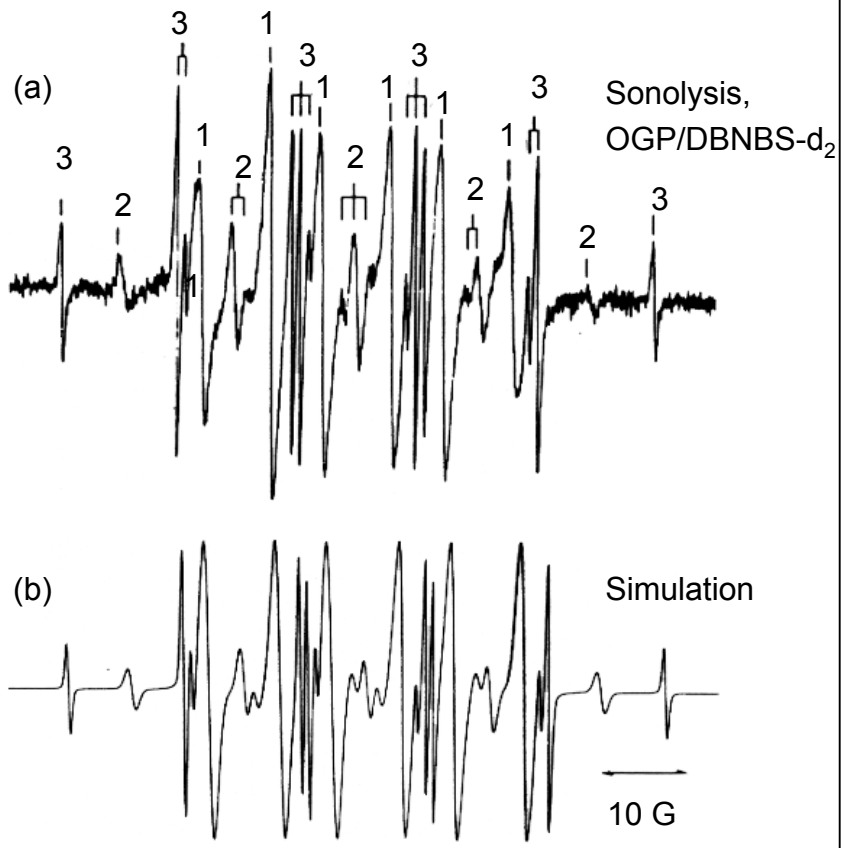

Figure 9: (a) EPR spectra following sonolysis of aqueous OGP solutions in the presence of DBNBS-d_2. A simulation of (a) is shown in (b). 1 = •CH; 2 = •CH_2; 3 = •CH_3

[•C-($R_1R_2R_3$)] radicals. Each component in the EPR spectrum was quantified. The results of this are shown in Figure 10 of the following slide.

*Alegria, A. E.; Lion, Y.; Kondo, T.; Riesz, P. *J. Phys. Chem.*, **1989**, *93*(12), 4908-4913.

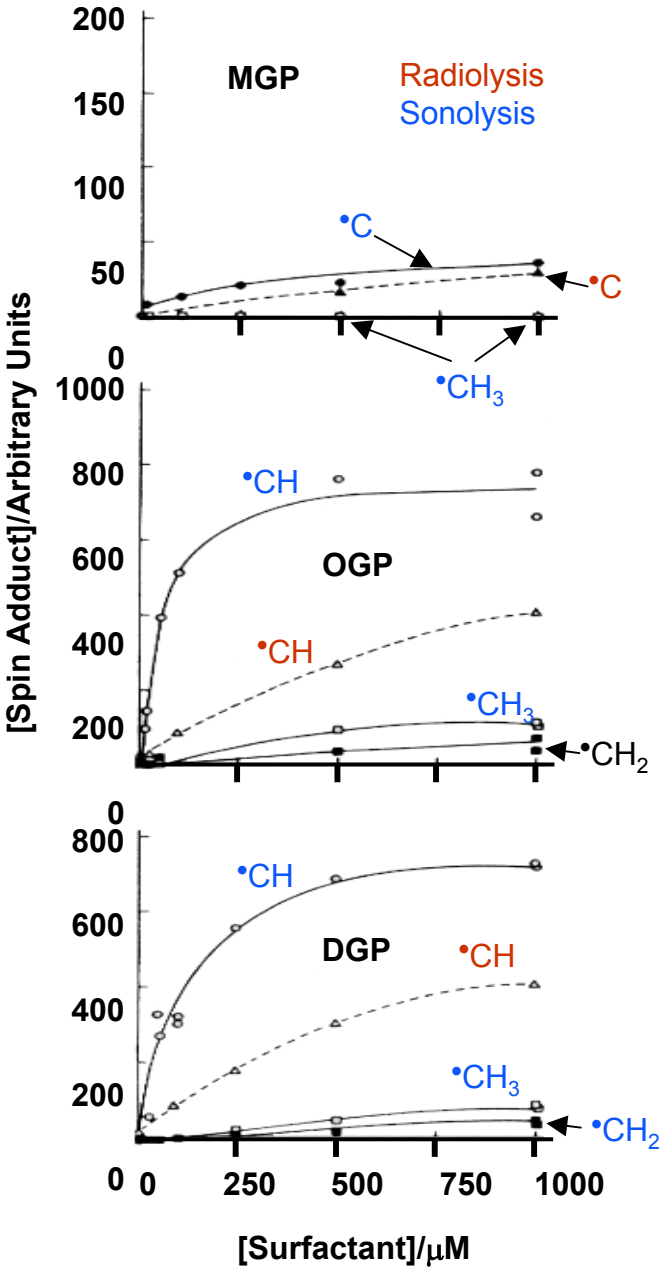

It can be seen from Figure 10 that as the bulk solution concentration of surfactant is increased up to 1000 μM, the yield of carbon centered radicals increases up to a plateau value. Interestingly, the relative yield of carbon centered radicals was much smaller for the non-surfactant analogue (MGP) compared to the surfactants, OGP and DGP. In fact, methyl radicals could be detected at bulk solution concentrations as low as 250 μM for OGP and DGP, which was 500 fold lower than the concentrations of MGP required (data not shown). This was the first definitive evidence using EPR and spin trapping experiments to show that solutes with surfactant properties can accumulate more readily at the gas/solution interface of violently oscillating cavitation bubbles.

Figure 10: DBNBS-d_2 spin adduct yield following sonolysis as a function of surfactant concentration. [DBNBS-d_2] = 3 mM, sonolysis was conducted under argon gas and radiolysis under N_2O.

Alegria, A. E.; Lion, Y.; Kondo, T.; Riesz, P.
J. Phys. Chem., **1989**, *93*(12), 4908-4913.

Recently, we have used DBNBS-d_2 to study the accumulation and decomposition mechanisms of n-alkyl chain possessing ionic, zwitterionic and non-ionic surfactants at the gas/solution interface of cavitation bubbles. A summary of the groups of surfactants used is shown below, where x = total number of carbon atoms in the n-alkyl chain:

Figure 11:

Ionic	$CH_3(CH_2)_{x-1}$—	OSO_3^-
	$CH_3(CH_2)_{x-1}$—	OSO_2^-
Zwitterionic	$CH_3(CH_2)_{x-1}$—	$^+N(CH_3)_2(CH_2)_3OSO_2^-$
Non-ionic	$CH_3(CH_2)_{x-1}$—	$(OCH_2CH_2)_8OH$

Typical EPR spectra observed following sonolysis of ionic, zwitterionic and non-ionic surfactants are shown in Figure 12. The spectra of Figure 12 provide information about the mechanism of decomposition of non-volatile surfactants. For example, the zwitterionic and non-ionic surfactants, having more complex head group structures, gave higher yields of $^{\bullet}CH_3$ radicals compared to the ionic surfactants.

Sostaric, J. Z.; Riesz, P.
J. Am. Chem. Soc., **2001**, *123*, 11010-11019.

An interesting result, considering that the n-alkyl chain of the surfactants is pointing toward the interior of the hot spot.

Figure 12: EPR spectra following sonolysis of argon saturated, aqueous solutions of DBNBS (8.2 mM) and (a) SDS (3 mM, ionic); (b) C_8-Zwitterionic (10 mM); (c) C_{10}-non-ionic (0.3 mM).

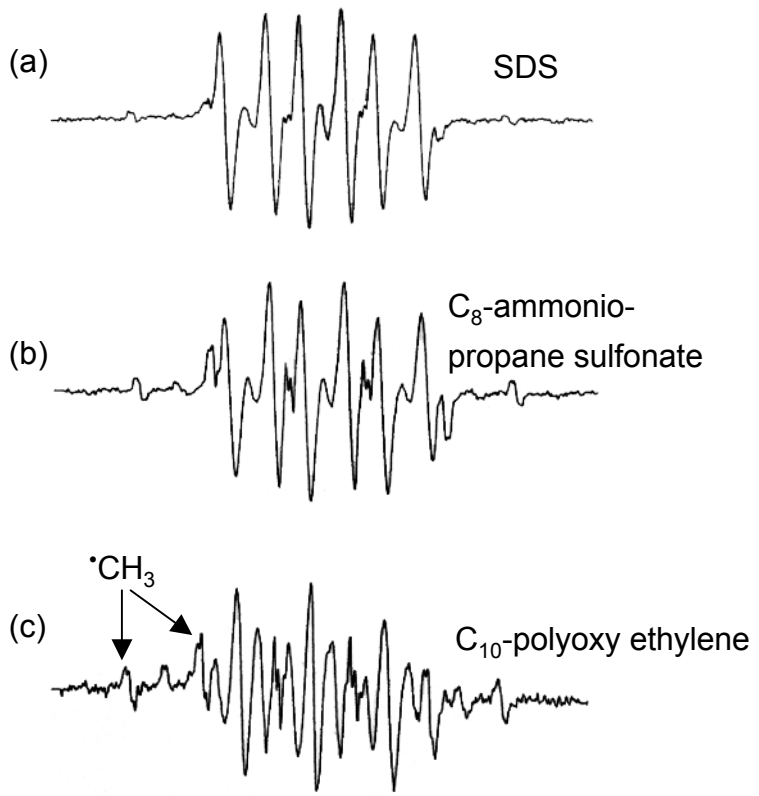

vi) Free Radical Intermediates in Sonodynamic Therapy:

The biological effects of ultrasound are summarized in Figure 13:

Figure 13:

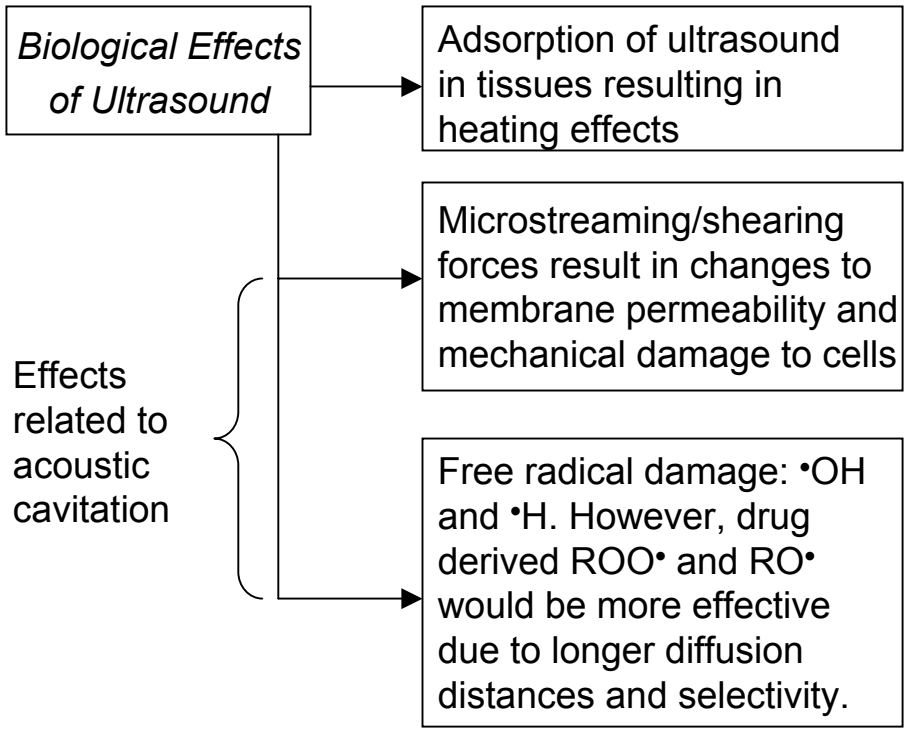

*Misik, V.; Riesz, P. *Ann. N.Y. Acad. Sci*, **2000**, *899*, 335-348

Sonodynamic therapy is a promising new modality for cancer treatment based on the synergistic effect on cell killing by the combination of a drug (sonosensitizer) and ultrasound. Relevant research in sonodynamic therapy is listed in Table 1 (on the following slide). However, the mechanism by which cell killing is enhanced in the presence of sonosensitizers has not been fully elucidated. Our research has focussed on determining the type of radicals formed following sonolysis of known sonosensitizers.
Jeffers et al. (*J. Acoust. Soc. Am.*, **1995**, *97*, 669-676) showed that N,N-dimethyl formamide (DMF) had a synergistic effect on the killing of HL-60 human promyelocytic leukemia cells using ultrasound. Using the spin trap DBNBS in nitrogen saturated aqueous solutions, the formation of $^{\bullet}CH_3$ and $^{\bullet}CH_2N(CH_3)CHO$ were detected*. In air saturated solutions, these carbon centered radicals reacted with oxygen to form the corresponding peroxyl radicals which were spin trapped with 5,5-dimethyl-1-pyrroline-N-oxide (DMPO)*. Studies of this type* were helpful in contributing to our understanding of the mechanism of sonodynamic therapy.

Table 1. Synergistic effect of drugs and ultrasound in cancer research (references to follow)

Compound	Experimental System	Reference
Nitrogen Mustard	Inoculation of mice with mouse leukemia L1210 cells	[1]
Daunomycin	Rats bearing Yoshida sarcoma	[2]
Adriamycin	Rats bearing Yoshida sarcoma	[2]
	Fibrosarcoma (RIF-1) or melanoma (B-16) bearing mice	[3]
	V79 Chinese hamster fibroblast cells	[4]
	CHO and MCF-7 WT cells	[5]
	Uterine cervical squamous cell carcinoma implanted in the cheek pouch of Syrian hamster	[5]
4'-O-tetrahydropyranyl-adriamycin	Sarcoma cells	[6]
Diaziquone	CHO and MCF-7 WT cells	[5]
	Uterine cervical squamous cell carcinoma implanted in the cheek pouch of Syrian hamster	[5]
Hematoporphyrin	Mice bearing sarcoma 180	[7]
Photofrin	HL-60 cells	[8]
	Adult T-cell leukemia cells	[9]
	Mice bearing colon 26 carcinoma	[10}
Ga-porphyrin ATX-70	Isolated sarcoma 180 cells	[11]

Table 1. Synergistic effect of drugs and ultrasound in cancer research (continued)

Compound	Experimental System	Reference
Various porphyrins	Murine leukemia	[12]
Rose bengal	Sarcoma 180	[13]
DMF, DMSO Methylformamide	HL-60 human promyelocytic leukemia cells	[14]
Photofrin II	Sarcoma 180 cells	[15]
ATX-70	Mice bearing colon 26 carcinoma	[16]
ATX-70/F11-39 monoclonal antibody conjugate	Human gastric carcinoma *in vitro*	[17]

References – sonodynamic therapy

1. KREMKAU, F.W., J.S. KAUFMANN, M.M. WALKER, P.G. BURCH & C.L. SPURR. (1976). Ultrasonic enhancement of nitrogen mustard cytotoxicity in mouse leukemia. *Cancer* **37**: 1643-1647.
2. YUMITA, N., A. OKUMURA, R. NISHIGAKI, K. UMEMURA & S. UMEMURA. (1987). The combination treatment of ultrasound and antitumor drugs on Yoshida Sarcoma. *Jpn. J. Hyperthermic Oncol*. **3**: 175-182.
3. SAAD, A.H. & G.M. HAHN. (1989). Ultrasound enhanced drug toxicity on chinese hamster ovary cells in Vitro. *Cancer Research* **49**: 5931-5934.
4. LOVEROCK, B.P., G. TER HAAR, M.G. ORMEROD & P.R. IMRIE. (1990). The effect of ultrasound on the toxicity of adriamycin. *Brit. J. Radiol*. **63**: 542-546.
5. HARRISON, G.H., E.K. BALCER-KUBICZEK & H.A. EDDY. (1991). Potentiation of chemotherapy by low-levels of ultrasound. *Int. J. Radiat. Biol.* **59**: 1453-1466.
6. YUMITA, N., KANEUCHI, M., OKANO, Y., NISHIGAKI, R., UMEMURA, K., UMEMURA, S. (1999). Sonodynamically induced cell damage with 4'-O-tetrahydropyranyladriamycin, THP. *Anticancer Research* **19**: 281-284
7. YUMITA, N., R. NISHIGAKI, K. UMEMURA & S. UMEMURA. (1990). Synergistic effect of ultrasound and hematoporphyrin on sarcoma 180. *Jpn. J. Cancer Res*. **81**: 304-308.
8. TACHIBANA, K., N. KIMURA, M. OKUMURA, H. EGUCHI & S. TACHIBANA. (1993). Enhancement of cell killing of HL-60 cells by ultrasound in the presence of the photosensitizing drug Photofrin II. *Cancer Letters* **72**: 195-199.
9. TACHIBANA, K., T. UCHIDA, S. HISANO & E. MORIOKA. (1997). Eliminating adult T-cell leukaemia cells with ultrasound. *Lancet* **349**: 325.

References – sonodynamic therapy

10. YUMITA, N., NISHIGAKI, R., UMEMURA, S. (2000). Sonodynamically induced antitumor effect of Photophrin II on colon 26 carcinoma. *J. Cancer Res Clin Oncol* **126**: 601-606

11. UMEMURA, S., N. YUMITA & R. NISHIGAKI. (1993). Enhancement of ultrasonically induced cell damage by a gallium-porphyrin complex, ATX-70. *Jpn. J. Cancer Res*. **84**: 582-588.

12. KESSEL, D., R. JEFFERS, J.B. FOWLKES & C. CAIN. (1994). Porphyrin-induced enhancement of ultrasound cytotoxicity. *Int. J. Radiat. Biol*. **66**: 221-228.

13. UMEMURA, S., YUMITA, N., UMEMURA, K., NISHIGAKI, R. (1999) Sonodynamically induced effect of rose bengal on isolated sarcoma 180 cells. *Cancer Chemother Pharmacol* **43**: 389-393

14. JEFFERS, R.J., R.Q. FENG, J.B. FOWLKES, J.W. HUNT, D. KESSEL & C.A. CAIN. (1995). Dimethylformamide as an enhancer of cavitation-induced cell lysis *in vitro*. *J. Acoust. Soc. Am*. **97**: 669-676.

15. YUMITA, N., UMEMURA, S., NISHIGAKI, R. (2000). Ultrasonically induced cell damage enhanced by photofrin II. Mechanism of sonodynamic activation. *In Vivo*, **14**: 425-429.

16. SASAKI, K., YUMITA, N., NISHIGAKI, R., SAKATA, I., NAKAJIMA, S., UMEMURA, S. (2001). Pharmacokinetic study of a gallium-porphyrin photo- and sono- sensitizer, ATX-70 in tumor bearing mice. *Jpn. J. Cancer Res.*, **92**:989-995.

17. ABE, H., KUROKI, M., TACHIBANA, K., LI, T. L., AWASTHI, A., UENO, A., MATSUMOTO, H., IMAKIIRE, T., YAMAUCHI, Y., YAMADA, H. ARIYOSHI, A. (2002), Targeted sonodynamic therapy of cancer using a photosensitizer conjugated with antibody against carcinoembryonic antigen. Anticancer Res., 22:1575-1580.

A synergistic effect of porphyrins and ultrasound on cell killing and on tumor bearing animals (Yumita, N. et al., *Jpn. J. Cancer Res.*, **1990**, *81*, 304-308) was discovered by Umemura and co-workers. Our research on the aqueous sonochemistry of porphyrin molecules has resulted in the identification of typical carbon centered radicals that are observed following the sonolysis of surface active organic solutes in aqueous solutions. This suggests that the sonodynamic effect in the presence of porphyrins could be due to a radical mechanism. An example of the EPR spectrum observed following sonolysis of ATX-C_7 in the presence of DBNBS-d_2 is shown in Figure 15.

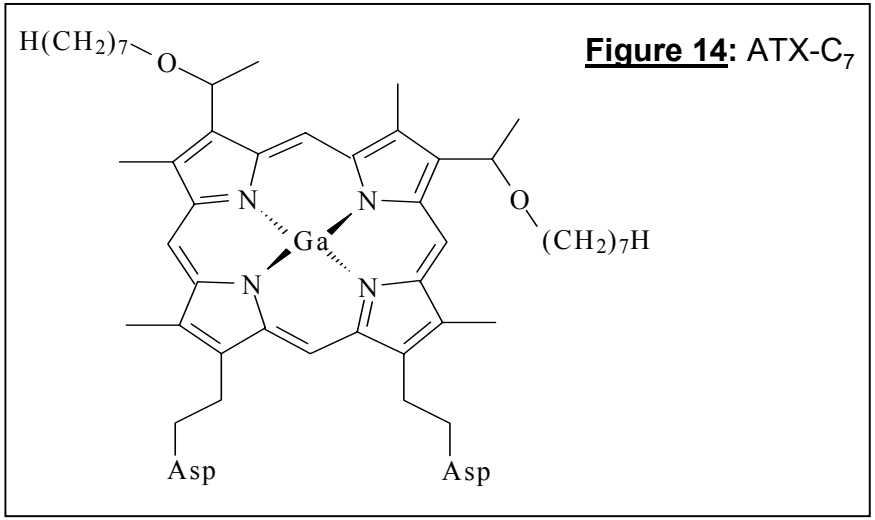

Figure 14: ATX-C_7

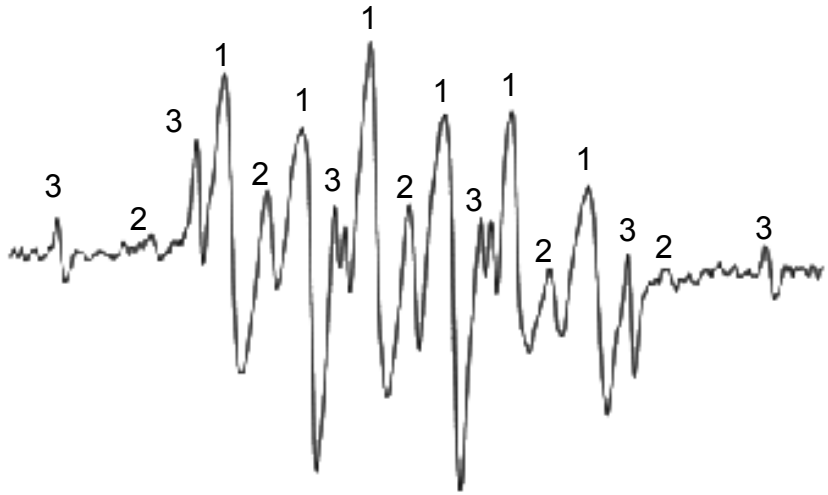

***Figure 15:** EPR spectrum following the sonolysis of argon saturated ATX-C_7 solutions in the presence of DBNBS-d_2. The lines in the spectrum are labeled: methyl (3), $-^{\bullet}CH_2$ (2) or $-^{\bullet}CH-$ (1) carbon radical spin adducts.

Misik, V.; Riesz, P. *Ann. N.Y. Acad. Sci*, **2000**, *899*, 335-348.

*Miyoshi, N.; Sostaric, J. Z.; Riesz, P. Unpublished results.

The work on basic sonochemistry, especially with regard to radical trapping reactions following the sonolysis of model surfactant systems and aqueous solutions of sonosensitizers has been useful in helping to elucidate the mechanism of sonodynamic therapy. A working hypothesis for sonodynamic therapy is shown in Figure 16. The non-volatile sonosensitizers undergo pyrolysis or radical scavenging reactions with •H and •OH at the gas/solution interface of collapsed cavitation bubbles. The intermediates (carbon centered radicals) react with oxygen to form peroxyl and alkoxyl radicals. These radicals have a much longer diffusion distance through the extracellular medium and are capable of attacking the allylic hydrogens of lipids in the plasma membrane, thus initiating lipid peroxidation chain reactions. In contrast, •H atoms and •OH radicals that diffuse from the hot spot to the extracellular medium cannot cause significant cellular damage, due to their short diffusion distances, as a result of their extremely high reactivities.

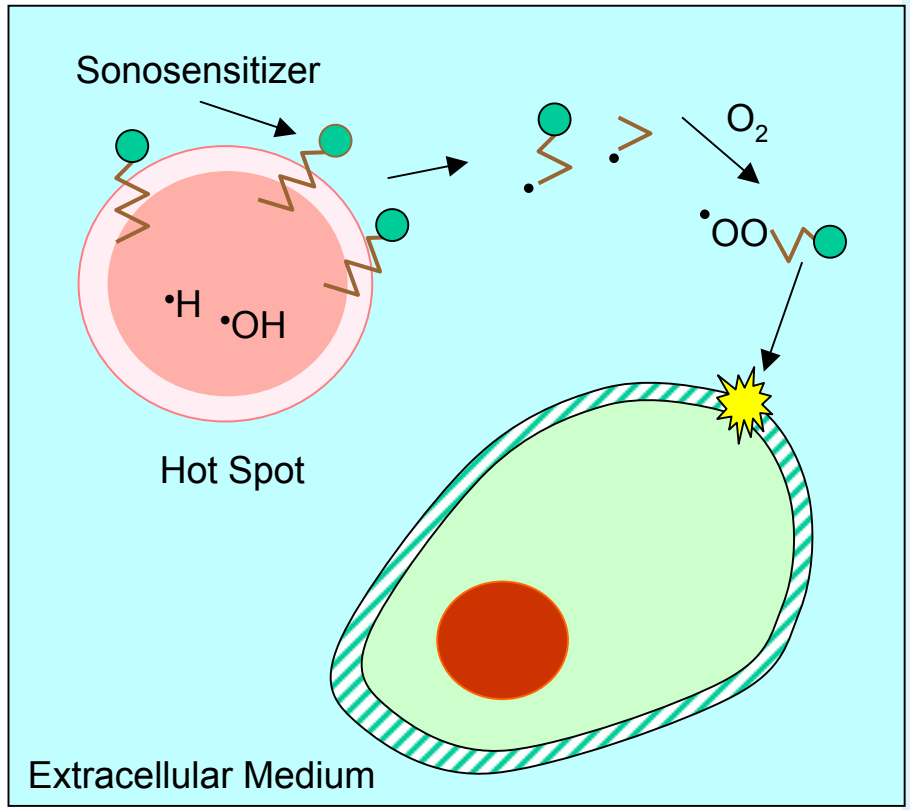

Figure 16: The mechanism of sonodynamic therapy (Not to scale)

Misik, V.; Riesz, P.
Ann. N.Y. Acad. Sci, **2000**, *899*, 335-348